

## A SENSITIVITY STUDY OF RESERVOIR AND GEOMECHANICAL PARAMETERS ON HYDRAULIC FRACTURING INITIATION AND PROPAGATION IN TIGHT FORMATIONS

Mohammad Tabaeh Hayavi, Mohammad Abdideh

*Department of Petroleum Engineering, Omidiyeh Branch, Islamic Azad University, Omidiyeh, Iran*

Received March 25, 2016; Accepted May 26, 2016

---

### Abstract

Hydraulic fracturing is a widely used stimulation technique in the petroleum industry for enhanced hydrocarbon recovery from low permeable reservoirs. Accurate knowledge of parameters affecting fracture initiation pressure provides essential information to assess the identification of fracture initiation zones and hydraulic fracture strategies as well as completion design requirements.

This paper presents the sensitivity of the reservoir and geomechanical parameters on fracture initiation pressure and geometry of propagated fractures for oil and gas wells drilled in tight formations. This study is conducted based on the linear poroelastic and Khristianovich-Geertsma-Deklerk (KGD) models.

The results indicate that the fracture initiation pressure increases with increasing the tensile strength of rock, poroelastic stress coefficient and reservoir pressure but decreases with increasing the Poisson's ratio, Biot's coefficient and horizontal stress anisotropy. The average fracture width increases with increasing the fracturing fluid viscosity and fracture half length but decreases with increasing the Poisson's ratio and Young's modulus.

Efficient prediction of initiation and propagation of hydraulically induced fractures are therefore essential for petroleum industries to undertake effective hydraulic fracture stimulation tasks.

**Keywords:** fracture initiation pressure; geomechanical parameters; average fracture width; linear poroelastic model- Biot's coefficient.

---

## 1. Introduction

Hydraulic fracturing has been used commercially as a stimulation technique in the petroleum industry. Such fracturing jobs are designed to stimulate production from reservoirs with low permeability. This often involves pumping large amounts of fluid and solids (proppants), thus creating long fractures filled with proppants. A massive hydraulic fracturing (MHF) job may exceed one thousand cubic meters of fluid and one million kilograms of proppant. The fracture thus creates a high-permeability flow channel towards the wellbore which has a large drainage area towards the low-permeability formation [1].

In the field of rock mechanics, hydraulic fracturing is the process of injecting pressured water into a sealed bare borehole to induce tensile fracture in the rock. This fracturing process is characterized by the formation, growth, and coalescence of microcracks as well as the initiation and development of macroscopic faults [2].

Hydraulic fracturing is widely used in the petroleum engineering, mining, and geotechnical industries. The most common application of this technology is enhancement of the fluid flow from oil, gas, and geothermal reservoirs in low permeability formations. Other applications of hydraulic fracturing include the underground disposal of waste drill cuttings, goafing and fault [3].

Hossain *et al.* [4] presents a generic model for prediction of hydraulic fracture initiation pressure, orientation and location of fractures on the wellbore wall. Based on influencing factors of the treatment condition and the seepage effect of fracturing fluid and the pore pressure, Zhou *et al.* [5] established the model of the stress distribution around the hydraulic

---

fractured wellbore, presented the predicting model of fracture initiation pressure and azimuth, and analyzed the effects of different in-situ stress on fracture initiation. Warpinski *et al.* [6] introduced the concept of altered stress fracturing whereby a hydraulic fracture in one well is reoriented by another hydraulic fracture in a nearby location. And then, Palmer *et al.* [7] presented the concept of induced stress that the initial differential stress can determine the stress reorientation in refracturing.

The dimension and propagation characteristics of a hydraulic fracture are important information in design of fracturing operations. Knowing the properties of reservoir rock, fracturing fluid, and the magnitude and direction of in situ stresses, one seeks an accurate prediction of the dimension (opening width, length, and height) of the hydraulically induced fracture for a given pumping rate and time. Many fracture models have been developed for this purpose. The initiation of a hydraulic fracture from a vertical wellbore and two-dimensional fracture propagation model are discussed in the following sections [8].

The breakdown pressure is defined as the pressure required not only for fracture initiation but early propagation, since the identification of the fracture initiation pressures has proved not to be sufficient to determine if a zone could be fractured or not. Field observations suggest that the breakdown pressure moves between the pressure requirements to overcome the minimum in-situ stress and the tensile strength of the materials, considering for both cases the additional pressure needed for early fracture extension. Based on these, lower and upper bounds can be determined through the definition of the profiles related to: (1) Minimum in-situ stress. (2) Pressure required to overcome the tensile strength (3) Early fracture extension pressure. The pressure requirements for fracture initiation are influenced not only by the far field stress but by the re-distribution of stresses around the well, tensile strength and mechanical properties of the materials [9]. This paper presents the effects of the reservoir and geomechanical parameters on fracture initiation pressure based on linear poroelastic model and geometry of propagated fractures using the Khristianovich-Geertsma-Deklerk (KGD) model.

## 2. Methodology

### 2.1. Construction of mechanical earth model

A Mechanical Earth Model (MEM) is an explicit description of the mechanical properties of the reservoir and overburden formations, including rock strength and elastic properties, the state of in-situ stresses and their direction as well as pore pressure. It forms the basis for any geomechanical analysis, such as hydraulic fracture design, wellbore stability analysis, sanding prediction evaluation, mechanical characterization of fractured formation, fault seal evaluation, reservoir compaction and subsidence evaluation, etc. Therefore, the reliability of hydraulic fracturing analysis largely relies on robustness of the MEM [10].

The field and laboratory data required for this study are provided from a number of production wells drilled in one of oil fields located in the south west of Iran. This oil field is one of the most important Iranian super giant oil fields, was discovered in 1956 and now has more than 450 producing wells. This oil field has an anticline structure 72 km long and 6 km wide with NW-SE trending symmetrical anticlinal, located in central part of north Dezful region. Its main reservoir is the Asmari formation and Bangestan Group with the production rate of 1000,000 barrels/day [11]. The Bangestan reservoir is one of the carbonate reservoirs in southern of Iran, providing approximately 5% of the total production of the southern oil field region. Because of a sufficient amount of oil in place and the good quality of porosity with low permeability and flowing capacity in some of the production layers, it is a good candidate for a hydraulic fracturing operation [12]. This reservoir includes the thick Sarvak limestone (300m to 1000m thick) of Cenomanian-Turonian age and the thinner Illam formation (50m to 200m thick) of Santonian age (Figure 1). These two reservoirs form a single reservoir in most of the Dezful Embayment and capped by the thick Gurpi/Pabdeh marls [13].

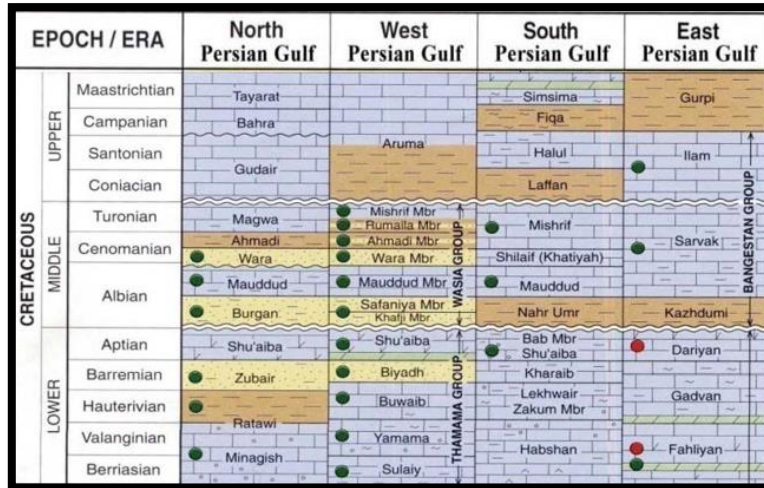


Figure 1 Simplified Stratigraphy of Bangestan Group in Persian Basin [14].

**2.1.1. Calculation of rock mechanical properties**

The mechanical properties of formations and dynamic elastic constants of subsurface rocks can be derived from the measurement of elastic wave velocities and density of the rock. Sonic logging and waveform analysis provide the means for obtaining continuous measurements of compressional and shear velocities. These data, in conjunction with a bulk density measurement, permit the in-situ measurement and calculation of the mechanical properties of the rock. The elastic moduli relationships, in terms of elastic wave velocities (or transit times) and bulk density can be calculated from following equations [15].

$$v_d = \frac{\frac{1}{2}(\frac{\Delta t_s}{\Delta t_c})^2 - 1}{(\frac{\Delta t_s}{\Delta t_c})^2 - 1} \tag{1}$$

$$E_d = \frac{\rho_b \left[ 3 - 4 \left( \frac{\Delta t_c}{\Delta t_s} \right)^2 \right]}{\Delta t_s^2 - \Delta t_c^2} \tag{2}$$

$$\alpha_B = 1 - \frac{K_B}{K_R} \tag{3}$$

$$K_B = \rho_b \left( \frac{1}{\Delta t_c^2} - \frac{4}{3\Delta t_s^2} \right) b \tag{4}$$

$$K_R = \rho_{gr} \left( \frac{1}{\Delta t_c^2} - \frac{4}{3\Delta t_s^2} \right) b \tag{5}$$

where:  $v_d$  is the dynamic Poisson's ratio;  $E_d$  is the dynamic Young modulus (psi);  $\alpha_B$  is Biot's coefficient;  $\Delta t_s$  is shear wave travel time (ft/s);  $\Delta t_c$  is compressional wave travel time (ft/s);  $k_B$  is dynamic bulk modulus (psi);  $K_R$  is the rock modulus (psi);  $\rho_b$  is the bulk density ( $gr/cm^3$ );  $\rho_{gr}$  is the grain density ( $gr/cm^3$ ); and "b" is the constant coefficient which is equal to  $1.34 \cdot 10^{10}$ .

For the Bangestan formation of mentioned oilfield, an equation developed for estimation of shear wave travel time by Nabaei *et al.* [16] was used:

$$\Delta t_s = 1.7891\Delta t_c + 7.622 \tag{6}$$

Dynamic data cannot directly be utilized to develop mechanical models. So, they should be first converted into static data through some calculation changes made and then used in geomechanical model [17]. Poisson's ratio and static Young's modulus are both calculated via the following relations in south west of Iran. The results show good conformity with laboratory data [18].

$$v_s = v_d \tag{7}$$

$$E_s = 0.4145E_d - 1.0593 \tag{8}$$

where  $v_s$  is the static Poisson's ratio and  $E_s$  is the static Young modulus (psi).

### 2.1.2. In-Situ stresses and pore pressure

In-situ stress magnitudes play a very important role in geomechanical analysis, and they are the most basic parameter inputs in analysis of hydraulic fracturing. Vertical stress is induced by the weight of the overlying formations. The vertical stress can be calculated by integration of rock densities from the surface to the depth of interest based on Eq. 9. In fact, density log can be used to calculate overburden stress [19].

$$\sigma_v = g \int_0^z \rho(z) dh \approx \bar{\rho}gz \quad (9)$$

where:  $\sigma_v$  is vertical stress (psi);  $z$  is depth of interest (ft);  $\rho(z)$  is the density as a function of depth ( $\text{gr/cm}^3$ );  $g$  is gravitational acceleration ( $\text{ft/s}^2$ ) and  $\bar{\rho}$  is the mean overburden density of rocks ( $\text{gr/cm}^3$ ).

Rocks of Bangestan formation have an average density of  $2.6 \text{ gr/cm}^3$ . By considering horizontal strain and deformation effect, Hooke's law can be applied to derive the horizontal stresses and strains relationships [19]. The following equations are obtained, and are used to calculate the minimum and maximum horizontal stresses with tectonic strain effects [20].

$$\sigma_h = \frac{v_s}{1-v_s} (\sigma_v - \alpha_B P_p) + \alpha_B P_p + \frac{v_s E_s}{1-v_s^2} \varepsilon_1 + \frac{E_s}{1-v_s^2} \varepsilon_2 \quad (10)$$

$$\sigma_H = \frac{v_s}{1-v_s} (\sigma_v - \alpha_B P_p) + \alpha_B P_p + \frac{v_s E_s}{1-v_s^2} \varepsilon_2 + \frac{E_s}{1-v_s^2} \varepsilon_1 \quad (11)$$

where:  $\sigma_h$  is minimum horizontal stress;  $\sigma_H$  is maximum horizontal stress;  $P_p$  is pore pressure;  $\varepsilon_1$  and  $\varepsilon_2$  are strains due to tectonic forces in maximum and minimum directions and considered 1 and 1.5, respectively.

Based on drilling information pore pressure gradient in this formation is estimated 0.44 psi/ft.

### 2.1.3. Stress concentration around a wellbore at production condition

The stress concentration around a well drilled in an isotropic, elastic medium under anisotropic in-situ stress condition (Maximum and minimum horizontal stresses are different) was described by the Kirsch equations. The general expressions for the stresses at the wellbore wall for a deviated well in the production situation are [1]:

$$\begin{aligned} \sigma_r &= P_{wf} \\ \sigma_\theta &= \sigma_x^\circ + \sigma_y^\circ - 2(\sigma_x^\circ - \sigma_y^\circ)\cos 2\theta - 4\tau_{xy}^\circ \sin 2\theta - P_{wf} + B(P_{wf} - P_r) \\ \sigma_z &= \sigma_z^\circ - v_s [2(\sigma_x^\circ - \sigma_y^\circ)\cos 2\theta + 4\tau_{xy}^\circ \sin 2\theta] + B(P_{wf} - P_r) \\ \tau_{\theta z} &= 2(-\tau_{xz}^\circ \sin \theta + \tau_{yz}^\circ \cos \theta) \end{aligned} \quad (12)$$

$$\tau_{rz} = 0; \tau_{r\theta} = 0$$

where:  $\sigma_r$  is the radial stress;  $\sigma_\theta$  is the tangential (hoop) stress;  $\sigma_z$  is the axial stress induced around a wellbore;  $P_{wf}$  is the bottomhole flowing pressure;  $P_r$  is reservoir pressure;  $\theta$  is measured from the azimuth of maximum horizontal stress (Degree) and  $B$  is the poroelastic stress coefficient defined as:

$$B = \frac{1-2v_s}{1-v_s} \alpha_B \quad (13)$$

The shear stresses at the wellbore wall are denoted  $\tau_{r\theta}$ ,  $\tau_{\theta z}$  and  $\tau_{\theta r}$ , while the in-situ stresses in (x, y, z) coordinate system, denoted  $\sigma_x^\circ$ ,  $\sigma_z^\circ$ ,  $\sigma_y^\circ$ ,  $\tau_{xy}^\circ$ ,  $\tau_{yz}^\circ$  and  $\tau_{xz}^\circ$ , and they are defined as [21]:

$$\begin{aligned} \sigma_x^\circ &= (\sigma_H \cos^2 \alpha + \sigma_h \sin^2 \alpha) \cos^2 i + \sigma_v \sin^2 i \\ \sigma_y^\circ &= \sigma_H \sin^2 \alpha + \sigma_h \cos^2 \alpha \\ \sigma_z^\circ &= (\sigma_H \cos^2 \alpha + \sigma_h \sin^2 \alpha) \sin^2 i + \sigma_v \cos^2 i \end{aligned} \quad (14)$$

$$\tau_{xy}^\circ = 0.5(\sigma_h - \sigma_H) \sin 2\alpha \cos i$$

$$\tau_{yz}^\circ = 0.5(\sigma_h - \sigma_H) \sin 2\alpha \sin i$$

$$\tau_{xz}^\circ = 0.5(\sigma_H \cos^2 \alpha - \sigma_h \sin^2 \alpha - \sigma_v) \sin 2i$$

where:  $i$  is wellbore inclination and  $\alpha$  is the azimuth angle due to the maximum horizontal stress ( $\sigma_H$ ) direction (Degree).

Figure 2 shows the stress transformation system in a deviated borehole where  $\alpha$  is the rotation angle around the  $z'$ -axis (measured from the  $x'$ -axis) and  $i$  is the rotation angle around the  $y'$ -axis (measured from the  $z'$ -axis).

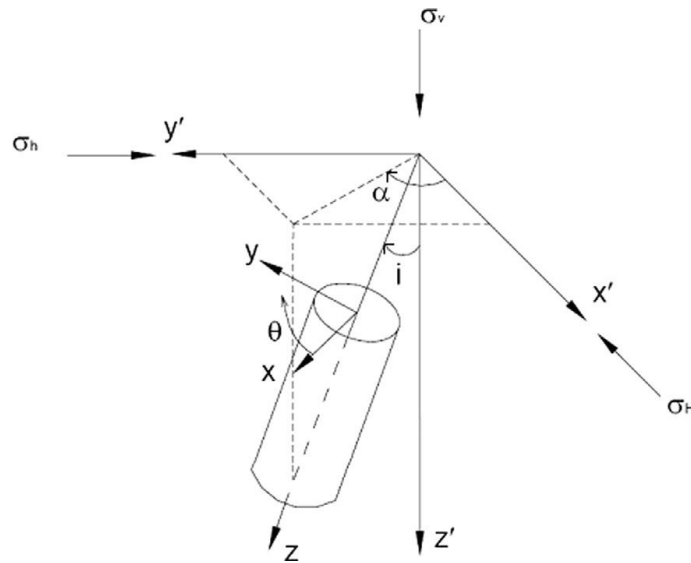


Figure 2. Stress transformation geometry for a deviated borehole [21]

The tensile failure known as fracturing is expected to happen at the wellbore wall and at the point of minimum tangential stress ( $\theta=0^\circ$ ) where the rock is under maximum tension [4]. For a vertical borehole, the inclination angle ( $i$ ) is set to zero and the  $x$ -axis is oriented, so that it coincides with the major horizontal principal stress axis (i.e.,  $\alpha = 0^\circ$ ). However, for a vertical well the minimum stress values will always be at  $\theta=0^\circ$  for any values of the in-situ stresses and Eqs. 12 become:

$$\begin{aligned} \sigma_r &= P_{wf} \\ \sigma_\theta &= 3\sigma'_h - \sigma'_H - P_{wf} + B(P_{wf} - P_r) \\ \sigma_z &= \sigma_v - 2\nu(\sigma'_H - \sigma'_h) + B(P_{wf} - P_r) \end{aligned} \quad (15)$$

The effect of reservoir pressure decline due to production can be accounted for in the above computation by updating the in-situ stresses. For a laterally large reservoir compared to its thickness, the change in vertical stress is considered negligible and therefore it is usually kept constant [22]. The maximum and minimum horizontal stresses are updated as follows, respectively:

$$\sigma'_H = \sigma_H - B\Delta P_r \quad (16)$$

$$\sigma'_h = \sigma_h - B\Delta P_r \quad (17)$$

$$\text{Where: } \Delta P_r = P_{ri} - P_{rc} \quad (18)$$

and  $\sigma'_H$  and  $\sigma'_h$  are the maximum and minimum horizontal stresses at current production condition, respectively.  $P_{ri}$  and  $P_{rc}$  are the initial and current reservoir pressures, respectively.

## 2.2. Hydraulic Fracture Initiation Pressure Model

According to the tensile strength criterion, the fracture initiates at the wellbore wall when a principal tensile stress exceeds the tensile strength of rocks. In an arbitrarily oriented wellbore, the radial stress,  $\sigma_r$  is one of the principal stresses. Other two principal stresses can be calculated by using the theory of combined stresses. Equations of these three principal stresses,  $\sigma_1$ ,  $\sigma_2$ , and  $\sigma_3$  can, thus, be written as follows [4]:

$$\begin{aligned} \sigma_1 &= \sigma_r \\ \sigma_2 &= 0.5[(\sigma_\theta + \sigma_z) + \sqrt{(\sigma_\theta - \sigma_z)^2 + 4\tau^2_{\theta z}}] \\ \sigma_3 &= 0.5[(\sigma_\theta + \sigma_z) - \sqrt{(\sigma_\theta - \sigma_z)^2 + 4\tau^2_{\theta z}}] \end{aligned} \quad (19)$$

where  $\sigma_1$  is the maximum principal stress;  $\sigma_2$  and  $\sigma_3$  are the intermediate and the minimum principal stresses, respectively.

From Eq. 19, it is clear that  $\sigma_3$  causes the highest tension (negative stress value) on wellbore wall. The first fracture will be initiate when  $\sigma_f$  satisfy the following criterion:

$$\sigma_3 - \alpha_B P_p \leq T_o \tag{20}$$

where  $T_o$  is the tensile strength of rock.

Substitution of Eqs. 15 into Eq. 19 and introducing the generated equation into the Eq. 20 gives the fracture initiation pressure (FIP) for a vertical wellbore:

$$P_{wf} = \frac{3\sigma_h - \sigma'_H + BP_{rc} + T_o}{1 + \alpha_B - B} \tag{21}$$

### 2.3. Estimation of Fracture Width with KGD Model

Assuming that a fixed-height vertical fracture is propagated in a well-confined pay zone (i.e. the stresses in the layers above and below the pay zone are large enough to prevent fracture growth out of the pay zone), Khristianovich and Zheltov [23] presented a fracture model as shown in Figure 3.

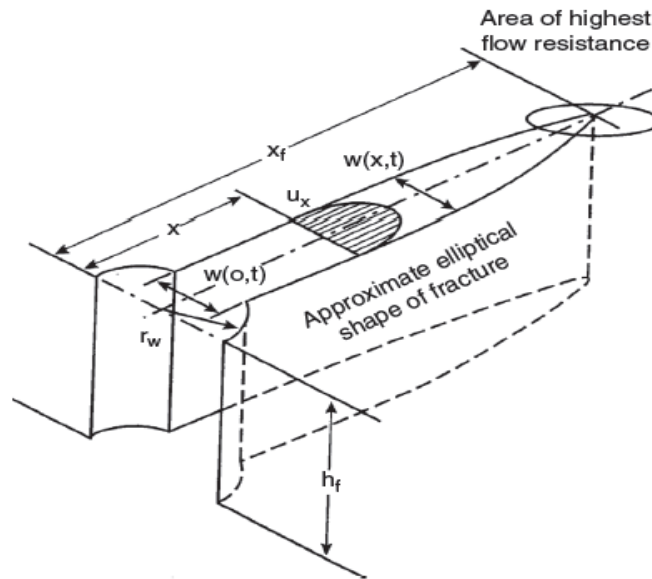


Figure 3 The KGD Fracture Geometry [23]

The model assumes that the width of the crack at any distance from the well is independent of vertical position, which is a reasonable approximation for a fracture with height much greater than its length. Their solution included the fracture mechanics aspects of the fracture tip. They assumed that the flow rate in the fracture was constant, and that the pressure in the fracture could be approximated by a constant pressure in the majority of the fracture body, except for a small region near the tip with no fluid penetration, and hence, no fluid pressure. This concept of fluid lag has remained an element of the mechanics of the fracture tip [24]. Geertsma and de Klerk [25] gave a much simpler solution to the same problem. The solution is now referred to as the KGD model. The average width of the fracture using the KGD model is expressed as [26-27]:

$$\bar{w} = 0.29 \left[ \frac{q_i(1-v_s)\mu_i x_f^2}{G_s h_f} \right]^{0.25} \left( \frac{\pi}{4} \right) \tag{22}$$

where:  $\bar{w}$  is the average fracture width (in);  $q_i$  is the pumping rate (bbl/day);  $h_f$  is the fracture height (ft);  $x_f$  is the fracture half length (ft);  $\mu_i$  is the viscosity of fracturing fluid (cp) and  $G_s$  is the static shear modulus (psi).

### 3. Results and Discussion

This section presents the sensitivity of the reservoir and geomechanical parameters on fracture initiation pressure and geometry of propagated induced fractures at the target depth (9000 ft) of Bangestan reservoir. Table 1 shows the geomechanical and reservoir properties

of this depth. In each subsection the influence of two different parameters on initiation pressure and geometry of induced fractures will be investigated.

Table 1-Geomechanical and reservoir properties of target depth

Geomechanical parameters	Value	Geomechanical parameters	Value
Vertical Stress ( $\sigma_v$ )	10 100 psi	Static Young's Modulus ( $E_s$ )	$6.10^6$
Maximum Horizontal Stress ( $\sigma_H$ )	8 100 psi	Tensile Strength ( $T_o$ )	500psi
Minimum Horizontal Stress ( $\sigma_h$ )	6 700 psi	Reservoir properties	
Biot's Coefficient ( $\alpha_B$ )	0.6	Initial Reservoir Pressure ( $P_{ri}$ )	6 000 psi
Static Poisson's Ratio ( $\nu_s$ )	0.3	Current Reservoir Pressure ( $P_{rc}$ )	5 100 psi

### 3.1. Effects of horizontal stress anisotropy ratio and poroelastic stress coefficient on FIP

Figure 4 shows the effects of horizontal stress anisotropy and poroelastic stress coefficient (B) on FIP. The horizontal stress anisotropy ratio is defined as

$$HSAR = \frac{\sigma'_H}{\sigma'_h} \tag{23}$$

As Figure 4 depicts, an increase in HSAR leads to decrease in the FIP in an invariable poroelastic stress coefficient. Also, it can be seen that increasing poroelastic stress coefficient tends to increase in the FIP.

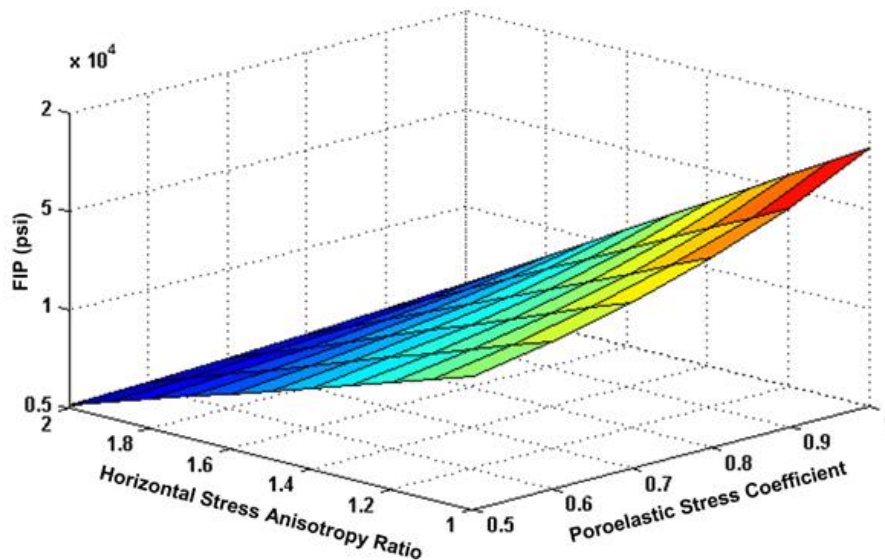


Figure 4 Effects of horizontal stress anisotropy ratio and poroelastic stress coefficient on FIP.

### 3.2. Effects of Poisson's ratio and Biot's coefficient on FIP

Figure 5 shows the influences of the Biot's coefficient and Poisson's ratio on FIP. It can be concluded that the FIP increases by decreasing the Poisson's ratio and/or Biot's coefficient. Furthermore, the sensitivity of Poisson's ratio on the FIP is very low.

### 3.3. Effects of reservoir pressure and tensile strength on FIP

Figure 6 displays the effects of reservoir pressure and tensile strength FIP. It can be concluded that the FIP decreases by decreasing the reservoir pressure and/or tensile strength.

### 3.4. Effects of Young's modulus and fluid viscosity on average fracture width

Figure 7 shows the effects of Young's modulus and fluid viscosity on average fracture width (AFW). Fig. 7 shows that increasing fluid viscosity tends to increase in the AFW. Also, decrease in Young's modulus leads to increase in AFW.

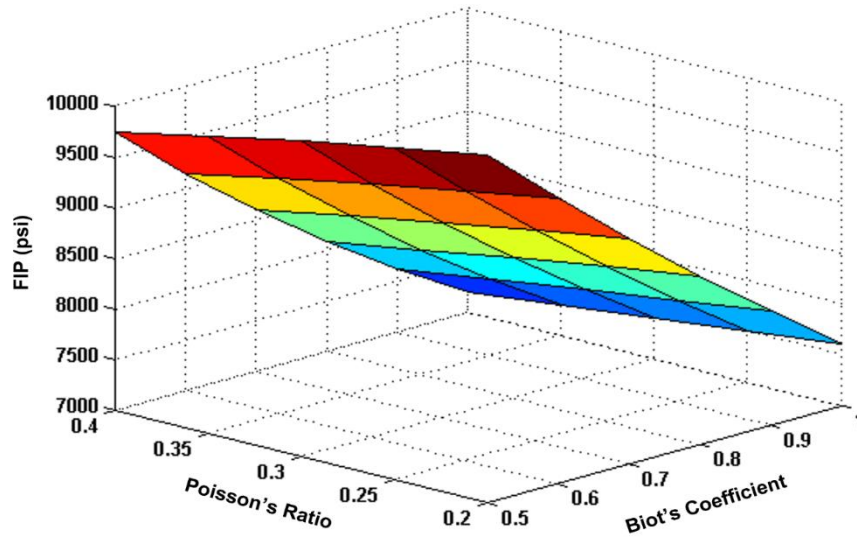


Figure 5. Effects Poisson's ratio and Biot's coefficient on FIP.

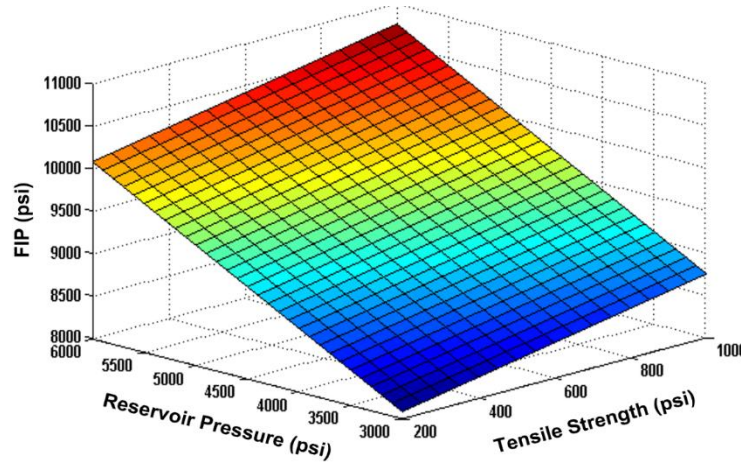


Figure 6. Effects reservoir pressure and tensile strength on FIP

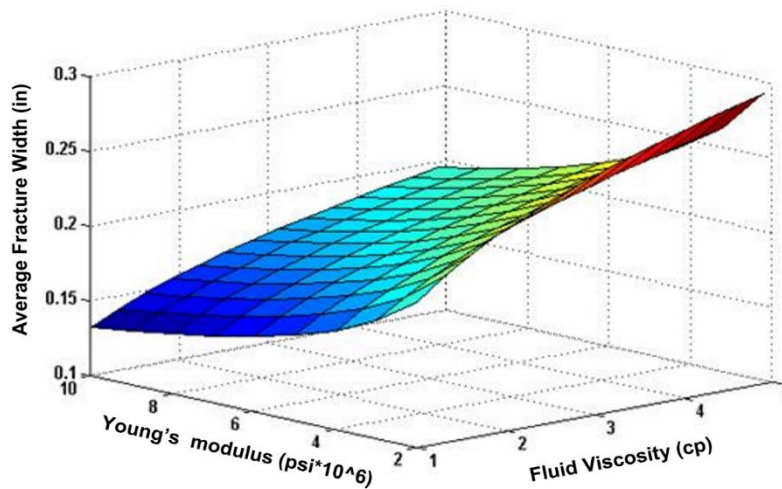


Figure 7. Effects Young's modulus and fluid viscosity on average fracture width

### 3.5. Effects of fracture half length and Poisson's ratio on average fracture width

Figure 8 indicates the influences of the fracture half length and Poisson's ratio on the AFW. It can be concluded that the AFW increases by increasing the fracture half length. On other hand, the Poisson's ratio has very small effect on AFW.

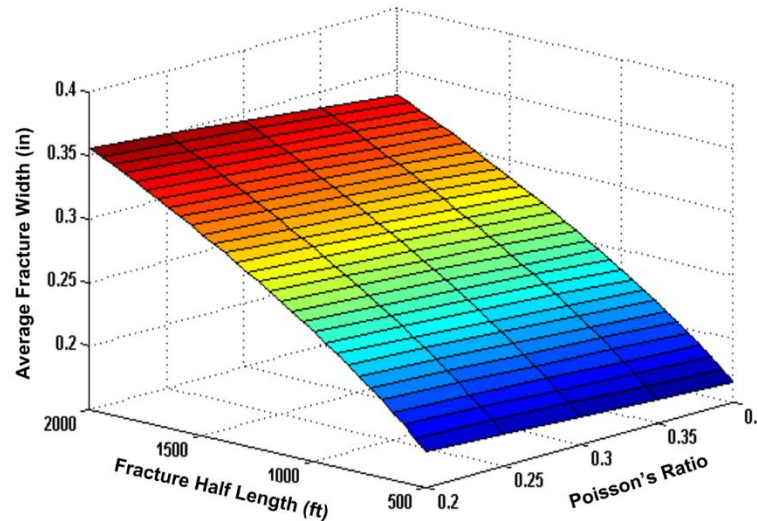


Figure 8. Effects fracture half length and Poisson's ratio on average fracture width

## 4. Conclusions

This paper presents the effect of reservoir and geomechanical parameters on fracture initiation pressure and average fracture width. The results indicate that:

1. The results indicated that the fracture initiation pressure increases with increasing the tensile strength of rock, poroelastic stress coefficient and reservoir pressure but decreases with increasing the Poisson's ratio, Biot's coefficient and horizontal stress anisotropy.
2. The average fracture width increases with increasing the fracturing fluid viscosity, and fracture half length but decreases with increasing the Poisson's ratio, and Young's modulus.
3. The effect of Poisson's ratio on fracture initiation pressure and average fracture width is very low.

## References

- [1] Fjær E, Holt RM, Horsrud P, Raaen AM, Risne A. Petroleum Related Rock Mechanics, 2nd edition Elsevier, Amsterdam. 2008.
- [2] Andreev G. Brittle failure of rock materials test results and constitutive models. Balkema, Rotterdam.1995.
- [3] Li L, Meng Q, Wang S, Li G, Tang TA. Numerical investigation of the hydraulic fracturing behavior of conglomerate in Glutenite formation, Acta Geotechnica, 2013, 47:110-119.
- [4] Hossain MM, Rahman MK, Rahman SS. A comprehensive monograph for hydraulic fracture initiation from deviated wellbores under arbitrary stress regimes. SPE 54360, In: Proceedings of the SPE Asia Pacific Oil and Gas Conference and Exhibition, 20-22 April 2011, Jakarta, Indonesia.
- [5] Zhou DY, Guo JC, Zhao JZ, Deng Y. Study of fracture initiation of the extended reach wells with open hole completion. Journal of Southwest Petroleum Institute, 2002, 24(6): 32-35.
- [6] Warpinski R, Norman F, Branagan R, Paul T. Altered-Stress Fracturing. Journal of Petroleum Technology. 1989, 41(9): 990-997.

- [7] Palmer ID. Induced stresses due to propped hydraulic fracture in coalbed methane wells, SPE 25861 presented at Low Permeability Reservoirs Symposium, 26-28 April 1993, Denver, Colorado.
- [8] Yew CH, Li L. *Mechanics of Hydraulic Fracturing*, 2nd edition Elsevier, Amsterdam, 2015.
- [9] Chavez J, Mjeni M, Briner A. Formation Breakdown Prediction for the Implementation of Hydraulic Fracturing on a HPHT Tight Gas Reservoir in Oman, SPE 164012. In: Proceedings of the SPE Middle East Unconventional Gas Conference and Exhibition, 28–30 January 2013, Muscat, Oman.
- [10] Mohiuddin MA, Najem MN, Al-Dhaferi YR, Bajunaid HA, Al-Khafji F. Geomechanical Characterization of a Sandstone Reservoir in Middle East—Analysis of Sanding Prediction and Completion Strategy. SPE 120049. In: Proceedings of the SPE Annual Technical Conference and Exhibition, 15–18 March 2009, Bahrain.
- [11] Motiei H. *Petroleum geology of Zagros-1*. Geological Survey of Iran (in Farsi), 1995 pp: 589-595.
- [12] Ashoori S, Abdideh M, Yahagh M. Investigation of hydraulic fracturing operation and fracture propagation simulation in reservoir rock *Geomechanics and Geoengineering*, 2014, 103(3): 203-211.
- [13] Rabbani AR, Bagheri TR. Hydrocarbon Source Rock Evaluation of the Super Giant Ahwaz Oil Field, SW Iran *Australian Journal of Basic and Applied Sciences*, 2010, 4(5): 673-686.
- [14] Hassanzadeh G, Kobraei M, Ahanjan A, Bagheri TR, Rashidi M, Khaleghi M. Petroleum System Analysis Using Geochemical Studies, Isotope and 1D Basin Modeling in Hendijan Oil Field, SW Iran IPTC 14797, In: Proceedings of the International Petroleum Technology Conference, 7–9 February 2011, Bangkok, Thailand.
- [15] Alipour TV, Mirzaahmadian Y. Investigation of Sand Production Onset: A New Approach Based on Petrophysical Logs, SPE 150529, In: Proceedings of the SPE Annual Technical Conference and Exhibition, 15–17 February 2010, Louisiana.
- [16] Nabaiei M, Shahbazi K, Shadravan A, Moazzeni MR. Artificial Neural Network Modelling Enhances Shear Wave Transit Time, SPE 12158, In: Proceedings of the SPE Annual Technical Conference and Exhibition, 16-20 November 2009, Kish Island,
- [17] Abdideh M, Fathabadi MR. Analysis of stress field and determination of safe mud window. *J. Petrol Explor. Prod. Technol.* 2013, 3: 105–110.
- [18] Wang HF. *Theory of linear poroelasticity*, Princeton University Press, 2000, Princeton.
- [19] Perchikolaee SR, Shadizadeh SR, Shahryar K, Kazemzadeh S. Building a Precise Mechanical Earth Model and its Application in Drilling Operation Optimization: A Case Study of Asmari Formation in Mansuri Oil Field. SPE 132204, In: Proceedings of the SPE Annual Technical Conference and Exhibition, 8–10 June 2010, Louisiana.
- [20] Al-Qahtani M, Rahim Z. A Mathematical Algorithm for Modeling Geomechanical Rock Properties of the Khuff and Pre-Khuff Reservoirs in Ghawar Field. SPE 68194, In: Proceedings of the SPE Annual Technical Conference and Exhibition, 17-20 March 2001, Bahrain.
- [21] Al-Shaabi S, Al-Ajmi A, Al-Wahaibi A. Three dimensional modeling for predicting sand production. *J Petrol Sci Eng.* 2013, 103: 348-363.
- [22] Rahman K, Khaksar A, Kayes K, Helix K. Minimizing Sanding Risk by Optimizing Well and Perforation Trajectory Using an Integrated Geomechanical and Passive Sand-Control Approach. SPE 116633, In: Proceedings of the SPE Annual Technical Conference and Exhibition, Colorado, USA, 21–24 September 2008, Bahrain.
- [23] Khristianovich SA, Zheltov YP. Formation of vertical fractures by means of highly viscous liquid. In: Proceedings of the SPE Fourth World Petroleum Congress held in Rome, Section II. 1955, pp. 579–586.

- [24] Guo B, Lyons W, Ghalambor A. Petroleum Production Engineering, ISBN: 0750682701, Elsevier Science & Technology, 2007.
- [25] Geertsma J, de Klerk F. A rapid method of predicting width and extent of hydraulic induced fractures. J. Petroleum Technol. 1996, 21: 1571–1581.
- [26] Peters KE, Cassa MR. Applied Source Rock Geochemistry In: The Petroleum System. 1994– 800-825.
- [27] Zhikai L, Shunli H, Daihong G, Hongling Z. Hydraulic Fracture Initiation While Staged Fracturing for Horizontal Wells, IPTC 16508, In: Proceedings of the International Petroleum Technology Conference, 26–28 March 2013, Beijing, China.

---

*\*Corresponding Author's Email: m.hayavi2013@gmail.com, Tel : +98 939 183 5971*